2026 IEEE International Conference on Robotics and Automation (ICRA 2026)
June 1-5, 2026. Vienna, Austria

Closed-Loop Multimodal Sensory Training Enhances the Proprioceptive-Motor Pathway: Low-Load Automaticity and Fine Motor Control

Qian Cheng, Zhouhaotian Yin, and Yuan Liu

Abstract—**Designing reliable upper-limb human-machine interfaces (HMIs) with low attentional demand requires strengthening the proprioceptive-motor pathway (PMP). We propose a closed-loop multimodal sensory training that maps three robot joint angles to six bidirectional electrotactile channels and combines visual fading with degrees-of-freedom (DoF) progression to shift reliance from vision to tactile-proprioceptive guidance. The objective is low-load automaticity for supplemental cues and improved native-limb fine motor control. Twenty right-handed adults completed a six-day protocol. Using synchronized kinematics and EEG, we evaluated electrotactile-driven tasks: eyes-closed continuous tracking and static posture reproduction, dual-task posture reproduction with serial subtraction, reversed-mapping generalization, and a proprioceptively constrained maze. Training produced robust gains under tactile-proprioceptive dominance: errors decreased (~30%) and response time shortened. Under dual-task load, posture error and response time decreased while correct subtractions increased and mistakes decreased, supporting low-load automaticity of electrotactile decoding. Although group-level β-event-related desynchronization (ERD) changes were not significant, contralateral ERD reductions and post-movement beta rebound (PMBR) enhancements during tactile decoding were consistent with reduced cortical effort and emerging automatic control. Performance generalized to reversed mapping, and maze completion time decreased significantly, evidencing improved fine motor control. These findings show that closed-loop vision-tactile-proprioceptive integration offers a compact, reproducible route to PMP enhancement, enabling low-load automaticity and finer control, with actionable design targets for prosthetics, exoskeleton rehabilitation, and vision-limited teleoperation.**

I. Introduction

Designing upper-limb human-machine interfaces (HMIs) that operate with low attentional demand requires strengthening the proprioceptive-motor pathway (PMP) and integrating multimodal feedback beyond vision. Artificial somatosensory channels, especially electrotactile and vibrotactile cues, can augment or partially substitute proprioception, thereby reducing cognitive load and stabilizing closed-loop control [1]. Research in multimodal HMI indicates that intuitive mappings and progressive training are prerequisites for reliable operation [2], while neurophysiological studies identify β-band activity as a marker of efficient sensorimotor processing and internal-model utilization [3].

A growing body of evidence shows that structured proprioceptive training improves perceptual and motor performance across tasks and populations [4]. Work on vibrotactile motor learning further indicates that effective augmentation depends on design levers such as stimulus mapping, sensor placement, and temporal scheduling [5]. With supplemental tactile cues and extended practice, accuracy and temporal efficiency improve [6]; moreover, the choice of mapping (joint space vs. task space) substantially shapes continuous-tracking performance [7]. Under stronger coupling, artificial touch can integrate near-optimally with vision [8] and even restore functional grip-force control via neural pathways [9]. In practice, tactile feedback is advancing toward deployable utility in robot-assisted surgery and is increasingly embedded in human-centric, multimodal HMI, including wearable and teleoperation systems [2], [10], [13].

Nevertheless, the transition of noninvasive artificial-feedback systems to real-world use remains constrained in three ways. First, functional gains outside the lab are often inconsistent due to unintuitive mappings and information complexity that elevate cognitive load [1], [5], [7], [13]. Second, many protocols rarely examine generalization to new mappings or task constraints, leaving uncertain whether learners acquire transferable internal structure [11]. Third, group-level neural evidence for efficiency gains is limited, even though β-band ERD or PMBR are theoretically linked to error-based learning, contextual inference, and post-movement stabilization [3], [12], [14], [15]. These gaps motivate closed-loop, multimodal approaches explicitly targeting low-load automaticity and fine motor control, together with multidimensional evaluation [4], [5].

Motivated by these gaps, we propose a closed-loop multimodal sensory training paradigm designed to enhance the PMP while minimizing attentional demand. Joint angles from a three-DoF robotic arm are encoded into six electrotactile channels (bidirectional per joint). Training pairs visual fading with DoF progression to reweight feedback reliance from vision toward tactile–proprioceptive guidance and to promote low-load automaticity and fine motor control [1–3], [11], [12].

*Research supported by the National Key Research and Development Program of China (2023YFC3603800, 2023YFC3603801), National Natural Science Foundation of China (62273251), Research Project of State Key Laboratory of Mechanical System and Vibration (MSV202418).

Q. Cheng is with Academy of Medical Engineering and Translational Medicine, Tianjin University, Tianjin, 300072, China (e-mail: qqiancheng@tju.edu.cn).

Z. Yin is with Academy of Medical Engineering and Translational Medicine, Tianjin University, Tianjin, 300072, China (e-mail: yinzhouht@tju.edu.cn).

Y. Liu is with Academy of Medical Engineering and Translational Medicine, Tianjin University, Tianjin, 300072, China (corresponding author, e-mail: ryanliu@tju.edu.cn).

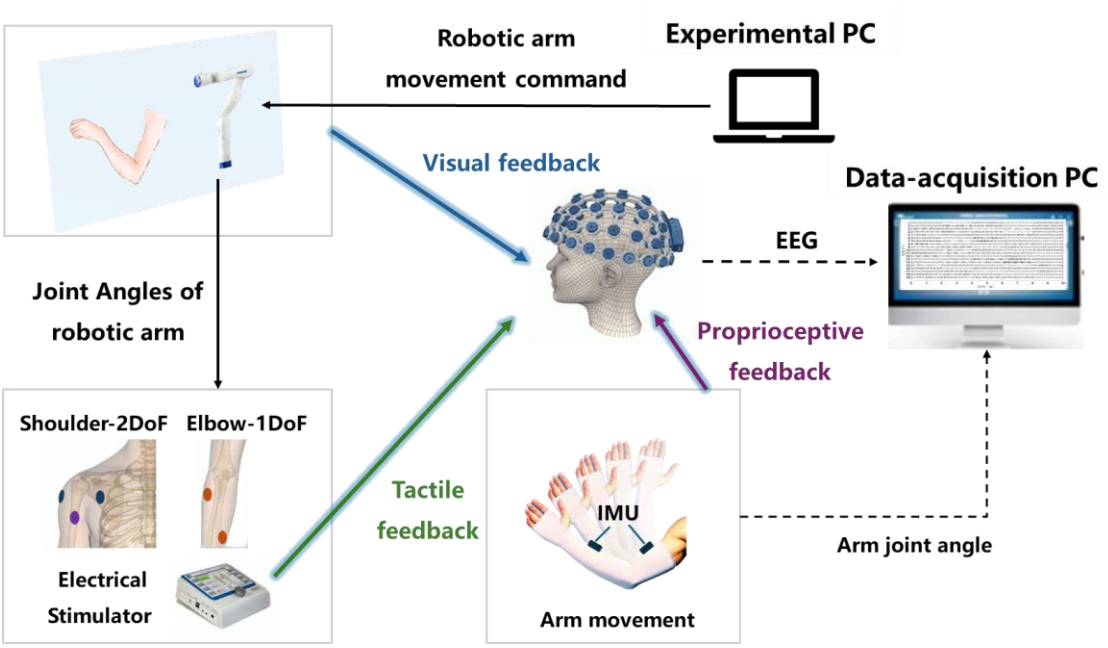

Figure 1. An experimental system integrating mechanical arms, electrical stimulators, and multimodal feedback of visual, tactile, and proprioceptive senses.

The efficacy of this paradigm is examined with synchronized kinematics and EEG across electrotactile-driven tasks: eyes-closed continuous tracking and static posture reproduction, dual-task posture reproduction with serial subtraction, reversed-mapping generalization, and a proprioceptively constrained maze. We hypothesize that training will reduce trajectory or posture errors and response time, facilitate low-load automaticity under cognitive load, and enable generalization under mapping reversal; we further expect β-band ERD or PMBR to provide supportive neural context consistent with more efficient cortical processing [6–9], [12]. These expectations align with contemporary sensorimotor-learning theory and emphasize fine motor control gains alongside PMP enhancement.

In summary, we present a closed-loop electrotactile training scheme that is grounded in visual fading and DoF progression and targets low-load automaticity, fine motor control, and PMP enhancement. By mapping robotic joint angles to six-channel electrotactile cues and leveraging vision-tactile-proprioceptive integration, the paradigm offers an actionable engineering route for upper-limb HMIs in prosthetics, exoskeleton rehabilitation, and vision-limited teleoperation. This route is consistent with the contributions summarized in the abstract.

II. Method

A. Experimental System

We built a multimodal, closed-loop platform to test whether sensorimotor training strengthens the proprioceptive-motor pathway. As shown in Fig. 1, the system comprised an experimental host, a data-acquisition host, a 7-DoF robotic arm, a multichannel electrical stimulator, inertial measurement units (IMUs), and an electroencephalography (EEG) module. The robotic arm provided standardized visual feedback, while the electrical stimulator delivered electrotactile cues. The cues encoded location and amplitude online from robotic joint angles. Participants actively tracked these cues to elicit proprioceptive feedback. All components were integrated into a timing-synchronized, multimodal closed loop that co-delivers visual, tactile, and proprioceptive inputs for learning and assessment.

A Kinova Gen3 7-DoF serial-link arm was used, with three DoFs enabled to generate controlled upper-limb trajectories. The experimental host (Ubuntu 18.04, ROS Noetic) managed joint-space waypoints and real-time communication. The robotic arm executed randomized waypoints with onboard planning to produce smooth three-DoF motion. Joint angles were continuously streamed and logged as kinematic references.

Tactile stimulation was delivered by a RehaStim2 (Hasomed) via electrodes placed on the shoulder and elbow. The three DoFs were mapped in real time to six stimulation channels (bidirectional encoding per joint), encoding both direction and amplitude. Frequency was fixed at 50 Hz. This ensured temporal alignment between robotic motion and electrotactile cues, coupling artificial feedback with intrinsic proprioception.

Four IMUs (Noraxon Ultium Motion) were attached to the upper spine, lower spine, upper right arm, and right forearm to capture natural kinematics. EEG was recorded with a 64-channel cap (Neuracle). All signals were synchronized by PsychoPy triggers on the experimental host.

B. Experimental Design

Three joint axes were selected. These axes were shoulder horizontal adduction or abduction (joint 1), shoulder flexion or extension (joint 2), and elbow flexion or extension (joint 3). Together, they cover the upper-limb workspace and map directly to the three robotic DoFs (Fig. 2A). Electrodes were placed around these joints to enable an intuitive one-to-one

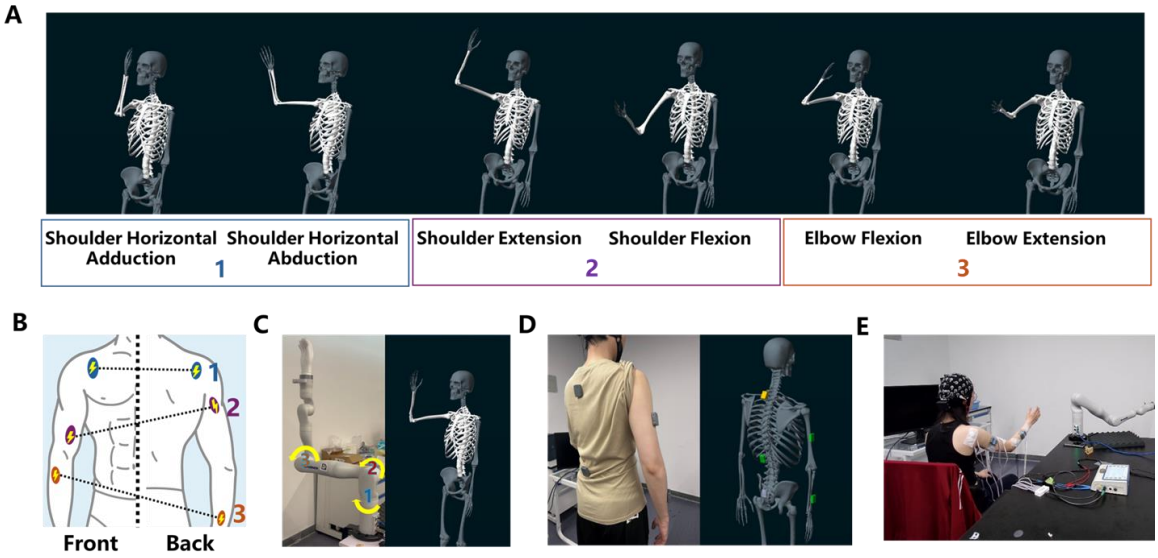

Figure 2. Experimental design and setup. (A) Three joints were selected: shoulder horizontal adduction/abduction (joint 1), shoulder flexion/extension (joint 2), and elbow flexion/extension (joint 3), mapped to three robotic DoFs. (B) Electrode placements around the three joints enabled intuitive one-to-one mapping between robotic movement and felt stimulation. (C) Neutral reference posture (90° trunk–arm–forearm); stimulation amplitude was zero at neutral and scaled with joint displacement. (D) Four IMUs attached at the upper spine, lower spine, upper arm, and forearm. (E) Experimental scene.

mapping between robotic motion and felt stimulation (Fig. 2B).

Taking a neutral position (with the angle between the trunk, upper arm, and forearm approximately 90°) as the reference (Fig. 2C), the offset amounts of each angle are all 0, and the electrical stimulation amplitude is 0. The range of motion for each joint angle of the robotic arm is similar to that of the human body height. Specifically, joint 1 ranges from -40 to 90 degrees (horizontal adduction-abduction) relative to the neutral position, joint 2 ranges from -90 to 45 degrees (shoulder flexion-extension), and joint 3 ranges from -90 to 50 degrees (elbow flexion-extension). Deviations in one direction activated the corresponding channel; the opposite deviation activated its paired channel. Stimulation amplitude was log-scaled with displacement (Weber-Fechner law) [16] to maintain sensitivity while avoiding discomfort. Up to six channels were supported, at 50 Hz. Individual thresholds (perceptual minimum and maximal comfortable intensity) were calibrated before experimentation.

According to the Noraxon upper-limb kinematic model, four IMUs were attached at the upper spine, lower spine, upper arm, and forearm (Fig. 2D). These sensors sampled at 100 Hz to record natural joint trajectories, which were subsequently compared with robotic movements to evaluate the decoding accuracy of stimulation feedback. Simultaneously, EEG signals were collected using a 64-channel cap at a sampling rate of 1000 Hz. All signals were time-locked with both stimulation and robotic events to guarantee temporal alignment.

The actual experimental scene is shown in Fig. 2E. The robotic arm was placed to the participant's right side, its workspace aligned with natural reach to emulate an auxiliary arm. Acquisition and stimulation devices were positioned proximally to minimize cable interference.

C. Procedure

Twenty right-handed participants (aged 18–27 years, with 8 male and 12 female) completed a six-day protocol: pre-test (Day 1), four days of progressive training (Days 2–5), and post-test (Day 6). Assessments targeted: (1) decoding of continuous motion and static posture feedback, (2) automatization of electrotactile decoding, (3) generalization under reversed mapping, and (4) proprioception-based fine motor control (Fig. 3A).

Before testing, participants completed a baseline task: following robotic trajectories with vision only (no stimulation) to quantify natural proprioceptive tracking error. This baseline was used to account for each participant's idiosyncratic mapping error in interpreting the correspondence between the robotic arm motion and their own movement range, and thus to isolate stimulation-related effects from pre-existing visuomotor or proprioceptive calibration differences.

In this study, a trial denotes one complete execution of the task following the unified timing sequence: 2 seconds rest, 5 seconds stimulation with motion or posture, then 3 s return to initial position (Fig. 3B). Right-arm kinematics and EEG were continuously recorded.

Evolution protocol (pre-post test)：

Continuous Tracking Test: Eyes-closed, real-time replication of robotic trajectories; stimulation varied continuously with displacement (3 sessions, each session contained 15 trials; 45 trials in total).

Static Posture Reproduction: Eyes-closed reproduction of terminal posture; 5 s of constant stimulation after the arm reached the end pose (2 sessions, each session contained 15 trials; 30 trials in total).

Dual-Task Posture Reproduction: Static posture reproduction plus serial subtraction by three (starting from a

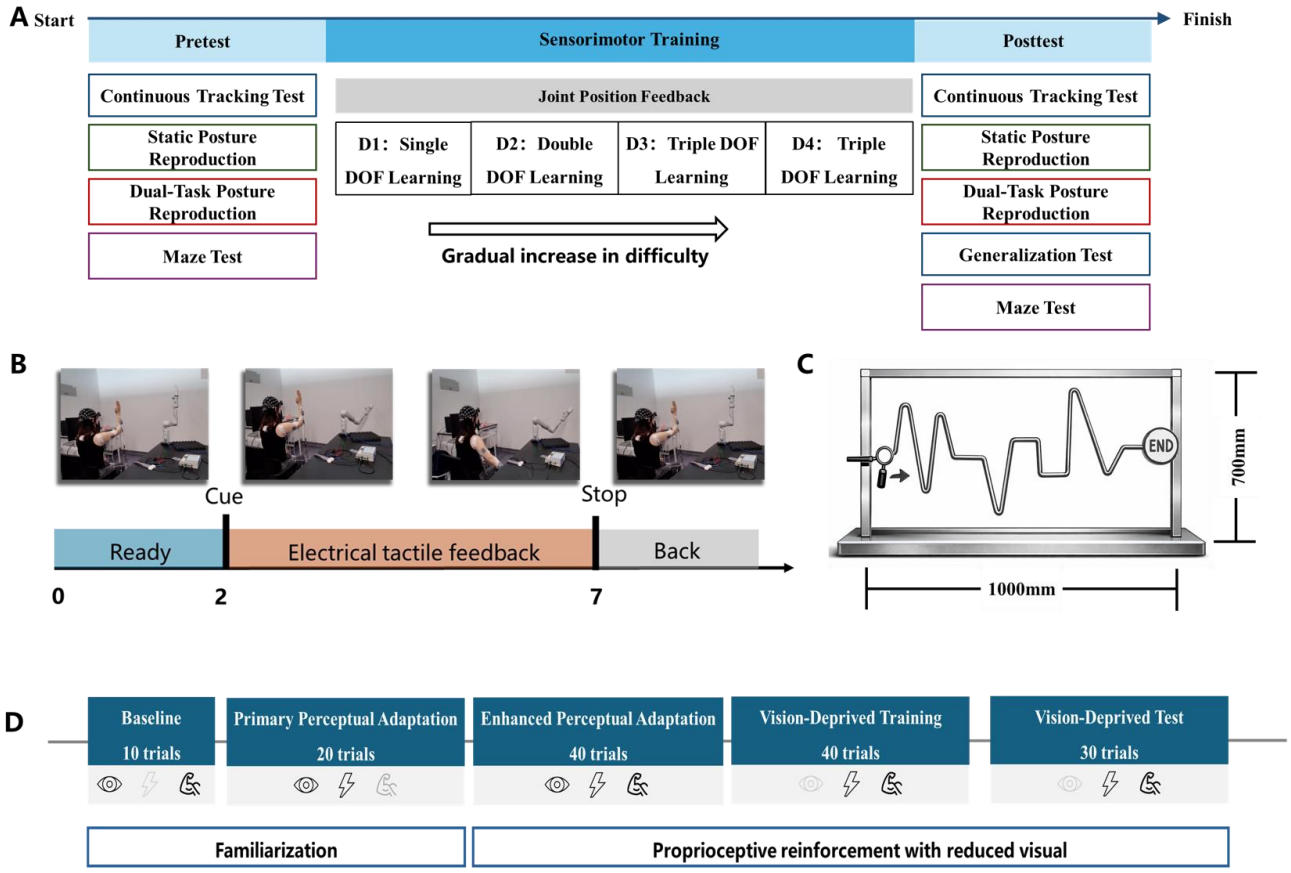

Figure 3. Experimental protocol. (A) Six-day protocol: pre-test (Day 1), progressive training (Days 2–5), and post-test (Day 6). (B) Trial structure: each trial consisted of 2 s rest, 5 s movement or posture with electrotactile feedback, and 3 s return. Right-arm kinematics and EEG were continuously recorded. (C) Maze task path diagram. (D) Training stages, the eyes represent visual feedback, the lightning represents electrical stimulation, and the arm represents motion tracking.

random 80–140 integer). Both motor and cognitive performance were recorded (2 sessions, each session contained 15 trials; 30 trials in total).

Generalization Test (post-test only): Reversed mapping where the neutral posture produced maximal stimulation and increasing displacement reduced intensity (2 sessions, each session contained 15 trials; 30 trials in total).

Maze Task: Participants guided a ring along a wire maze using only the right arm while keeping the trunk stationary (monitored by an experimenter and standardized verbal reminders). Any contact between the ring and the maze was treated as an error and required an immediate restart from the start position (Fig. 3C). Performance was quantified as completion time, defined as the elapsed time from movement onset to reaching the end point without contact; completion time was averaged across two valid trials.

Training protocol (Fig. 3D): Difficulty increased across days: Day 1 single-DoF, Day 2 two-DoF, Days 3-4 three-DoF. Each day comprised two stages: (i) Familiarization with combined visual and tactile feedback to establish mapping; (ii) Proprioceptive reinforcement with reduced visual cues to promote reliance on electrotactile input.

Training tasks included:

Primary Perceptual Adaptation: Observing robotic trajectories with visual and tactile cues to establish initial mapping.

Enhanced Perceptual Adaptation: Eyes-open trajectory tracking based on tactile cues, combining vision, touch, and proprioception to reinforce mapping.

Vision-Deprived Training: Replicating trajectories without vision, strengthening tactile-proprioceptive coupling. At trial end, participants opened eyes to compare robotic and natural endpoints, supporting error-based learning.

Progressive multi-DoF integration: Sequentially performing single-, double- and triple-DoF tasks, with increasing dominance of tactile feedback across days.

D. Data Analysis

Kinematics: Robotic and natural-arm trajectories were segmented by sync signals, aligned to stimulation onset, and baseline-corrected. Continuous tracking accuracy was quantified using multidimensional dynamic time warping (DTW) on the 3-joint angle vector, where DTW computes the minimum cumulative distance between two time series under a monotonic warping path that allows local time shifts, thereby capturing similarity despite differences in movement timing. Static posture accuracy was assessed by normalized root-mean-square error (RMSE), expressed as a percentage of

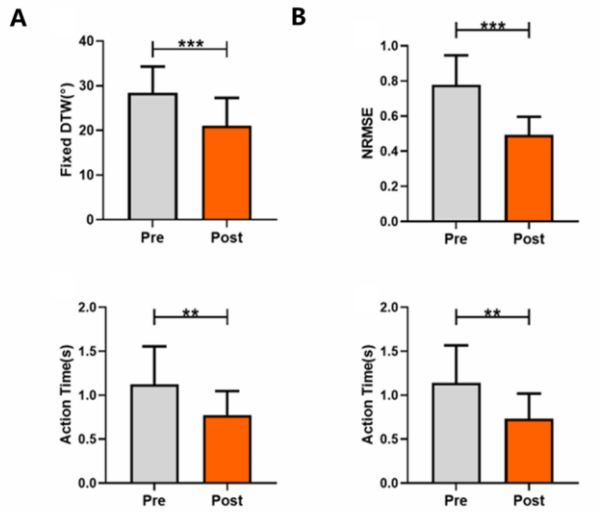

Figure 4. Training effects on electrotactile decoding. (A) Continuous tracking: cumulative joint-angle error (DTW) decreased by 25.9%, and action time shortened by 31.3%. (B) Static posture reproduction: normalized error (NRMSE) decreased by 36.7%, and action time shortened by 36.0%. * indicates < 0.05, ** indicates < 0.01, *** indicates < 0.001.

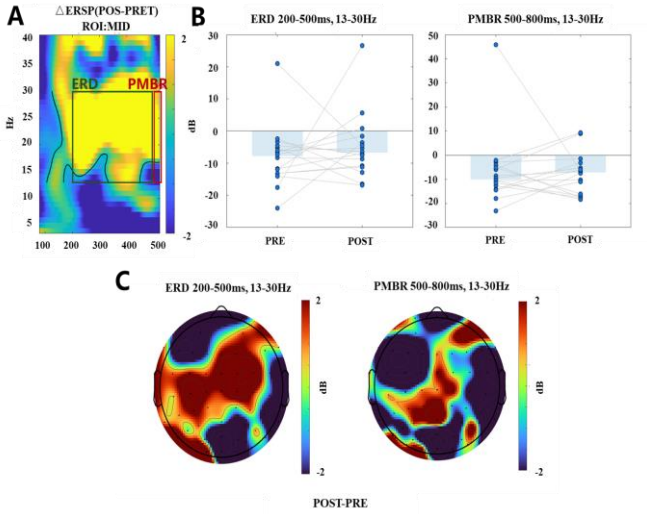

Figure 5. Group-level β-band ERSP in static posture paradigm. (A) Time–frequency map of ERSP (ΔPOST–PRE) in the contralateral sensorimotor ROI. (B) Individual changes in β-ERD and PMBR between pre- and post-training. (C) Topographical ΔERSP maps showing trends of reduced ERD and enhanced PMBR over central–sensorimotor regions.

each joint's range of motion. Response time was defined as the latency from stimulation onset to movement initiation.

EEG: Preprocessing used EEGLAB (v2023, MATLAB): 1–40 Hz band-pass, 500 Hz resampling, average re-reference, ICA with ICLabel for artifact removal, and spherical spline interpolation for bad channels. Data were epoched (−200–800 ms; −200–4000 ms). Time-frequency decomposition used Morlet wavelets (4–40 Hz). ERSPs were baseline-corrected relative to −200 to −50 ms and expressed in dB. Analyses focused on SML (FC3, C3, CP3) and MID (FCz, Cz, CPz). Within β (13–30 Hz), ERD (200–500 ms) indexed cortical engagement and PMBR (500–800 ms) indexed recovery; training-induced ERD/PMBR changes were interpreted as markers of proprioceptive-motor plasticity.

Behavior: In the dual-task, the number of correct subtractions and errors within 5 s indexed cognitive-motor interaction. In the maze task, completion time (mean of two attempts) indexed fine-motor transfer.

Individual metrics were compared pre- with post-training. Kinematic and behavioral measures (DTW, NRMSE, response time, subtraction counts/errors, maze time) used paired t-tests. EEG measures (ERD, PMBR) used Wilcoxon signed-rank tests. Significance was set at $p < 0.05$, with effect sizes (r) reported.

III. Result

Across all paradigms, the closed-loop robotic arm-electrotactile-proprioceptive training with visual fading and DoF progression improved kinematic accuracy, shortened response latency, and preserved performance under added cognitive load and mapping reversal. These effects indicate more efficient transformation of electrotactile cues into motor output within the proprioceptive-motor pathway.

Training markedly improved electrotactile decoding in both paradigms (Fig. 4). In continuous tracking, cumulative joint-angle error decreased by 25.9% ($p < 0.001$), with an average residual error of about 25%. Response time shortened by 31.3% (from 1.12 s to 0.77s, $p = 0.005$). In static posture reproduction, relative error decreased by 36.7% ($p < 0.001$) and response time by 36.0% (from 1.12 s to 0.73 s, $p < 0.001$), indicating more accurate and efficient decoding.

As shown in Fig. 5, group-level β-band ERSP changes were not significant in static posture paradigm (ERD, 200-500 ms: Z = -0.67, $p = 0.501$; PMBR, 500-800 ms: Z = -0.52, $p = 0.605$). Nevertheless, most participants showed a consistent pattern over the contralateral sensorimotor ROI: reduced ERD amplitude (less movement-related inhibition) and enhanced PMBR (stronger post-movement synchronization). ΔERSP maps in the β band exhibited positive shifts centered over central-sensorimotor regions. Although not significant at the group level, these trends align with behavioral gains and support the interpretation that training strengthened tactile-proprioceptive integration and improved cortical processing efficiency.

With static posture reproduction combined with serial subtraction, participants-maintained accuracy while becoming faster after training (Fig. 6A): posture error decreased by 20.8% ($p < 0.001$) and response time by 26.1% (from 0.81 s to 0.60 s, $p = 0.032$). Cognitive performance also improved (correct subtractions increased from 2.84 to 3.80, $p = 0.0015$; errors decreased from 0.21 to 0.063, $p = 0.02$), indicating increasing automatization of electrotactile decoding and reduced cognitive load under dual task demands.

Effects transferred to a reversed mapping. As shown in Fig. 6B, fixed DTW error improved from 30.2° (pre) to 22.1° (post, $p < 0.001$) and remained better than baseline in the generalized condition (25.0°, $p < 0.05$). Response time improved more strongly (from 1.73 s to 1.02 s, $p < 0.01$) and further shortened

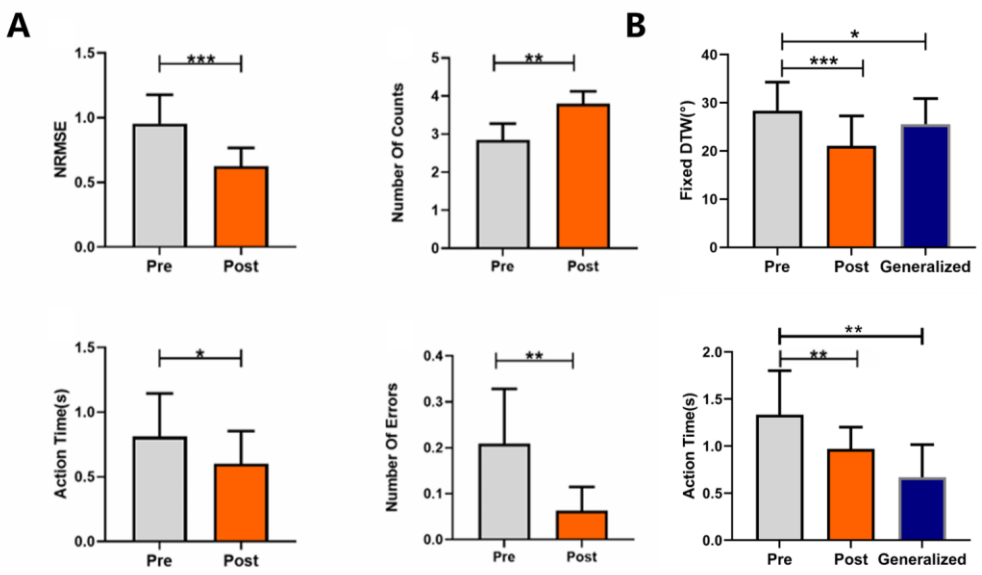

Figure 6. Dual-task and generalization effects. (A) Dual-task posture reproduction with serial subtraction: posture error decreased by 20.8% and response time by 26.1%. Cognitive performance improved, with more correct subtractions and fewer errors, indicating automatization of electrotactile decoding and reduced cognitive load. (B) Generalization under reversed mapping: fixed DTW error decreased from pre- to post-test and remained improved in the generalized condition. Response time shortened significantly from pre to postand further reduced under reversal, showing enhanced adaptability to new encoding rules. * indicates $p< 0.05$, ** indicates $p< 0.01$, *** indicates $p< 0.001$.

under reversal to 0.72 s ($p < 0.01$ vs. pre). Although generalized error was slightly larger than post-test, overall

performance remained significantly better than baseline, indicating improved adaptability to new encoding rules.

Training gains further transferred to fine motor control under proprioceptive constraints: post-test completion time was significantly shorter than pre-test (from 185s to 95 s, $p < 0.001$), indicating enhanced decoding of electrotactile cues and improved performance on complex, goal-directed actions, which consistent with strengthening of the proprioceptive-motor pathway.

IV. Discussion

This work demonstrates that a closed-loop multimodal sensory training paradigm is organized through visual fading and progressive degrees-of-freedom (DoF) progression. The paradigm reliably strengthens the proprioceptive-motor pathway (PMP) for upper-limb human-machine interfaces (HMIs) and significantly improves proprioception-based fine motor control. Across continuous tracking, static posture reproduction, dual-task posture plus serial subtraction, and reversed-mapping generalization, participants exhibited lower errors, shorter response times, improved cognitive-motor coexistence, and reduced maze completion time after training. Group-level EEG effects were not significant, yet β-band trends in contralateral sensorimotor regions provided supportive neural context. These trends included reduced ERD and enhanced PMBR, which were consistent with more efficient cortical processing. Collectively, these results indicate that the proposed interface and training schedule enhance the PMP, achieve low-load automaticity, and elevate fine motor control through vision-tactile-proprioceptive integration.

Training consistently reduced errors and shortened response times across continuous, static, dual-task, and reversed-mapping paradigms. This indicates that electrotactile feedback was not only perceived but also integrated as a reliable control signal for motor execution. In sensorimotor learning terms, repeated exposure reduces prediction error and calibrates internal forward and inverse models. This calibration enables faster and more accurate transformations from sensory cues to motor output [17]. The β-band EEG trends further suggest less widespread cortical desynchronization and stronger post-movement stabilization. Reduced ERD and enhanced PMBR are consistent with more efficient processing and the emergence of low-load automaticity. Functionally, these adaptations are manifested not only as decreased trajectory and pose error but also as gains in motor precision. These gains support fine motor control in proprioceptively constrained tasks such as the maze task.

In the dual-task paradigm, participants-maintained posture accuracy while improving subtraction performance. This pattern indicates that electrotactile decoding became increasingly automatic and less resource demanding. The training design used visual fading together with progressive DoF progression. This combination likely promoted sensory reweighting and shifted reliance from vision toward tactile-proprioceptive inputs while preventing overload. This aligns with principles of skill acquisition, where repeated and error-driven practice reduces the cognitive burden of control [17]. Importantly, this low-load automaticity coexisted with better fine motor control. This suggests that attentional resources freed by automatized decoding can be redeployed to stabilize precise movements under cognitive load. Such a property is advantageous for long-term HMI use.

Performance under reversed encoding remained significantly better than baseline. This result shows that participants learned not only specific stimulus-response mappings but also transferable internal structure. Such structural learning allows rapid adaptation to novel dynamics or rules because it abstracts invariant task features [18]. Practically, this means the interface and training foster a compact and reusable representation of tactile-proprioceptive mappings. Neural evidence provided supportive context. The enhanced PMBR trend aligns with reports that β rebound reflects confidence in internal-model estimates [19]. This reinforces the view that learners developed more stable internal representations.

The study was limited by a relatively homogeneous sample of young, right-handed adults. The training duration was short, and EEG findings were not significant at the group level. Future work should incorporate randomized controls, retention and savings tests, and perturbation paradigms that manipulate gain, delay, and direction. Future work should also include individualized psychophysics for stimulus scaling. Higher-density EEG with source localization and causal interventions such as TMS and tACS could directly test β-band mechanisms. Deployment in wearable, rehabilitation, and teleoperation contexts will further validate ecological utility for upper-limb human-machine interfaces.

V. Conclusion

This work demonstrates that closed-loop multimodal sensory training enhances the proprioceptive-motor pathway (PMP) under low attentional demand through vision-tactile-proprioceptive integration. The training maps three robot joint angles to six bidirectional electrotactile channels and pairs visual fading with degrees-of-freedom progression. Training produced lower errors, shorter response times, and significant gains in fine motor control. Electrotactile decoding exhibited low-load automaticity under dual-task conditions and generalized to a reversed mapping. Although group-level EEG effects were not significant, β-band trends, including reduced ERD and enhanced PMBR, provided supportive neural context consistent with more efficient cortical processing. Together, these outcomes align with sensorimotor-learning principles and offer a compact, reproducible framework for upper-limb human-machine interfaces (HMIs) in prosthetics, exoskeleton rehabilitation, and vision-limited teleoperation.

Acknowledgment

Research supported by the National Key Research and Development Program of China (2023YFC3603800, 2023YFC3603801), National Natural Science Foundation of China (62273251), Research Project of State Key Laboratory of Mechanical System and Vibration (MSV202418).

Figure 3C is a diagram drawn using ChatGPT based on actual electro-maze photos. It is used to remove the cluttered background and highlight the shape features. The shapes and sizes in this diagram are all real.

References

[1] J. W. Sensinger and S. Dosen, "A review of sensory feedback in upper-limb prostheses," Front. Neurosci., vol. 14, p. 345, 2020.

[2] T. Wang, S. Sun, C. Guo, M. H. Ang, and C. H. Yeow, "Multimodal human-robot interaction for human-centric robotics," Adv. Intell. Syst., vol. 6, no. 3, p. 2300359, 2024.

[3] J. Barone, A. Rossiter, and J. Marshall, "Understanding the role of sensorimotor beta oscillations," Front. Syst. Neurosci., vol. 15, p. 655886, 2021.

[4] L. Winter, M. Albisser, T. Berger, and S. Haller, "The effectiveness of proprioceptive training: A systematic review," Front. Rehabil. Sci., vol. 3, p. 830166, 2022.

[5] M. S. Islam, M. S. Hossain, and T. Ahmed, "Vibrotactile feedback in virtual motor learning: A systematic review," Appl. Acoust., vol. 188, p. 108587, 2022.

[6] V. A. Shah and D. Worrall, "Extended training improves the accuracy and efficiency of goal-directed reaching guided by supplemental vibrotactile feedback," Exp. Brain Res., vol. 241, no. 4, pp. 1017-1031, 2023.

[7] M. Pinardi, E. Meli, D. Prattichizzo, and N. Vitiello, "Comparing end-effector position and joint angle feedback for online robotic limb tracking," PLOS ONE, vol. 18, no. 5, p. e0285712, 2023.

[8] G. Risso, L. Marasco, F. Solazzi, M. Bergamasco, and A. Frisoli, "Optimal integration of intraneural somatosensory feedback with visual information," Sci. Rep., vol. 9, p. 8901, 2019.

[9] F. Clemente, L. D'Alonzo, G. Controzzi, I. Cipriani, M. C. Bianchi, and C. Cipriani, "Intraneural sensory feedback restores grip force control and motor coordination while using a prosthetic hand," J. Neural Eng., vol. 16, no. 2, p. 026034, 2019.

[10] J. Colan, F. L. García, A. M. Rivas-Blanco, and D. Blanco-Alonso, "Tactile feedback in robot-assisted minimally invasive surgery: A systematic review," Microsyst. Nanoeng., vol. 10, p. 23, 2024.

[11] J. B. Heald, M. Lengyel, and D. M. Wolpert, "Contextual inference underlies the learning of sensorimotor repertoires," Nature, vol. 600, pp. 489-493, 2021.

[12] H. Tan, C. Wade, and P. Brown, "Post-movement beta activity in sensorimotor cortex indexes confidence in the estimations from internal models," J. Neurosci., vol. 36, no. 5, pp. 1516-1528, 2016.

[13] C. Pacchierotti, S. Sinclair, M. Solazzi, A. Frisoli, V. Hayward, and D. Prattichizzo, "Wearable haptic systems for the fingertip and the hand: Taxonomy, review, and perspectives," IEEE Trans. Haptics, vol. 10, no. 4, pp. 580-600, 2017.

[14] E. Mastinu, F. Clemente, M. Sassu, M. M. Aszmann, and C. Cipriani, "Neural feedback strategies to improve grasping in upper-limb prostheses," Front. Neurosci., vol. 14, p. 736734, 2020.

[15] J. A. George, L. E. Kluger, D. M. Davis, et al., "Biomimetic sensory feedback through peripheral nerve stimulation improves dexterous use of a bionic hand," Sci. Robot., vol. 4, no. 32, p. eaax2352, 2019..

[16] G. W. Juette and L. E. Zeffanella, "Radio noise currents n short sections on bundle conductors (Presented Conference Paper style)," presented at the IEEE Summer power Meeting, Dallas, TX, June 22-27, 1990, Paper 90 SM 690-0 PWRS.

[17] D. M. Wolpert, J. Diedrichsen, and J. R. Flanagan, "Principles of sensorimotor learning," Nature Reviews Neuroscience, vol. 12, no. 12, pp. 739–751, 2011.

[18] D. A. Braun, A. Aertsen, D. M. Wolpert, and C. Mehring, "Motor task variation induces structural learning," Current Biology, vol. 19, no. 4, pp. 352–357, 2009.

[19] H. Tan, C. Wade, and P. Brown, "Post-movement beta activity in sensorimotor cortex indexes confidence in the estimations from internal models," Journal of Neuroscience, vol. 36, no. 5, pp. 1516–1528, 2016.